

## Position Isomerism on One and Two Photon Absorption in Multibranched Chromophores: A TDDFT Investigation

Claudine Katan,\*<sup>†,‡</sup> Mireille Blanchard-Desce,<sup>†</sup> and Sergei Tretiak\*,<sup>§</sup>

*Université Européenne de Bretagne, CNRS—Chimie et Photonique Moléculaires (CPM), Université de Rennes 1, 35042 Rennes, France, and Université Européenne de Bretagne, CNRS—Fonctions Optiques pour les Technologies de l'Information (FOTON), INSA de Rennes, CS70839, 35708 Rennes, France, and Center for NonLinear Studies (CNLS) and Center for Integrated NanoTechnologies (CINT), Los Alamos, New Mexico 87545, United States*

Received August 7, 2010

**Abstract:** Recently, branching and click chemistry strategies have been combined to design a series of optically active chromophores built from triazole moieties. These triazole-based multipolar chromophores have been shown to be promising candidates for two-photon absorption (TPA) transparency optimization in perspective of optical limiting in the visible region. In this work, the nature of one- and two-photon absorption properties in a family of triazole-based chromophores has been investigated using hybrid time-dependent density functional theory (TD-DFT). We use recent extensions of TD-DFT to determine nonlinear optical responses and natural transition orbitals to analyze the underlying electronic processes. Our results are also interpreted in the framework of the Frenkel exciton model. In agreement with experimental data, we found that introducing a triazole moiety into multibranched chromophores substantially modifies their optical behavior due to changes in electronic delocalization and charge-transfer properties between donating end groups and the branching center that can be controlled by the triazole ring. Structural conformations via modulation of the torsion between phenyl and triazole rings significantly alter the excited state electronic structure. Moreover, isomer positioning also greatly influences both linear and nonlinear optical responses such as TPA. Our theoretical findings allow elucidation of these differences and contribute to the general understanding of structure–property relations. Consequently, the interplay of donor/acceptor strength, triazole regiosomerism, and branching are shown to provide flexible means allowing for precise tuning of both linear and nonlinear optical responses, thus opening new perspectives toward synergic TPA architectures.

### I. Introduction

1,2,3-Triazole chemistry has recently gained renewed interest thanks to the click methodology offering far more ease of synthesis.<sup>1,2</sup> This has prompted synthetic effort to design novel molecular architectures in which the triazole moiety is assumed to play quite different roles, such as electron

donor,<sup>3</sup> electron acceptor,<sup>2,4,5</sup> active  $\pi$ -linker,<sup>6,7</sup> metal ligating entity,<sup>8,9</sup> or site-isolation group.<sup>10–12</sup> In particular, 1,2,3-triazole click chemistry has been explored in the field of small push–pull<sup>3,6,9,13</sup> and larger multipolar<sup>4,13</sup> chromophores up to dendrimers<sup>10</sup> and polymers with linear<sup>5</sup> or hyperbranched<sup>7,11,12</sup> polytriazole structures. In addition, 1,2,3-triazole has four points of attachment that allow for the design of various regiosomers which may show quite different behaviors.

This recent synthetic effort was partly driven by interest in their photophysical properties, which have long been overlooked and are still underdeveloped.<sup>6</sup> Recently, on the

\* Corresponding authors. E-mail: claudine.katan@insa-rennes.fr; serg@lanl.gov.

<sup>†</sup> CNRS Université de Rennes 1.

<sup>‡</sup> CNRS INSA de Rennes.

<sup>§</sup> CNLS and CINT.

basis of the assumption of electron-donating properties of triazole, ligation of this ring has been shown to effectively modulate the emission properties of coumarin, leading to increased fluorescence quantum yield by more than an order of magnitude.<sup>3</sup> Investigation of the photophysical properties of isomeric donor–acceptor-substituted 1,2,3-triazoles has also been reported.<sup>6</sup> It has been demonstrated both experimentally and theoretically that positioning of the donor and acceptor on the triazole ring results in important modulations of both transition energies and absorption intensities.<sup>6</sup> In the case of 1,4- and 1,5-linked hyperbranched polytriazoles, the different emission colors of the regiostructures were related to the differences in aggregation in the solid state.<sup>7</sup> On the basis of the site-isolation concept,<sup>14</sup> different hyperbranched polytriazoles have shown enhancement of their second-order nonlinear optical (NLO) responses overcoming the asymptotic dependence of electro-optic activity on chromophore density.<sup>10–12,15</sup> Finally, triazole-based multipolar<sup>4</sup> and functional poly(aryltriazole)s<sup>5</sup> have also been promising for their nonlinear optical properties, in particular, two photon absorption (TPA) capacity.

Indeed, among the numerous NLO processes, simultaneous absorption of two photons has gained increased attention over recent years<sup>16–21</sup> as it opens the way for improved and novel technological capabilities. This, in turn, led to the search for adequate functional materials with enhanced TPA responses. Thanks to their inherent modularity and potentially high TPA responses, conjugated organic molecular systems are of particular interest. From that perspective, the branching strategy has received much attention over recent years.<sup>16–18</sup> It relies on multibranch systems obtained by gathering several molecular units which are either of the dipolar<sup>21–31</sup> (also known as push–pull chromophores) or quadrupolar<sup>32–38</sup> type. In such nanoarchitectures, the interbranch coupling plays a central role. Depending on the nature and the strength of the interaction between the molecular units, optical properties such as TPA can show cooperative enhancement, additive behavior, or weakening. The interchromophore interactions are related to quite a few structural parameters: nature and length of the monomeric building blocks, number of chromophoric units, as well as nature of the branching center. All of these parameters will directly influence intermonomer distances and orientation and control the overall molecular symmetry.<sup>27</sup> Symmetry will, in turn, result in optically allowed and forbidden electronic transitions and drive oscillator strength redistribution among excited states (ESs) when going from the monomeric unit to the multichromophoric architecture. Besides the nature of the excitation, these parameters also influence the subsequent excitation energy transfer dynamics.<sup>39</sup>

Recently, branching and click chemistry strategies have been combined to design a series of TPA-active chromophores built from triazole moieties.<sup>4,13,40,41</sup> These triazole-based multipolar chromophores have been shown to be promising candidates for TPA transparency optimization from the perspective of optical limiting in the visible region. Obtained quadrupolar and three-branched chromophores have been shown to combine efficient synthesis, high solubility, intense absorption in the near UV region, full transparency,

high excited state lifetimes, and good TPA optical responses.<sup>4,13</sup> Moreover, emission wavelengths can be tuned, and excited state lifetimes can be significantly increased by increasing the polarity of the solvent. Related derivatives such as four-branched systems or position isomers have also been designed and experimentally investigated.<sup>40,41</sup> Experimental data reveal quite different behaviors as compared to the related quadrupolar, octupolar, or other multibranched compounds for both linear and NLO responses. As an example, when compared to similar three-branched systems also built by gathering branches through a triphenylamine central core, the triazole derivative deviates significantly. Indeed, no marked solvatochromic behavior of emission has been observed, while it is very effective for the quadrupolar analog<sup>13,40</sup> for which symmetry breaking in the relaxed excited state is thus clearly evidenced.<sup>42</sup> In addition, TPA cross sections of the three-branched chromophore still increase at 577 nm.<sup>4</sup> Thus, no maximum is observed near twice the one-photon absorption (OPA) wavelength (694 nm), as is usually the case.

To get a better understanding of triazole-based chromophores and to provide a deep physical insight into ongoing phenomena, theoretical calculations can be quite useful. Among the many different approaches ranging from simple few-state models up to high-level quantum methods (QM), the Frenkel exciton model has been shown to provide a valuable qualitative tool<sup>25,26,38,43–47</sup> with a few exceptions. Indeed, to be applicable, not only should the strength of the coupling (solely due to Coulomb interactions) between monomeric units be weak but the inherent nature (e.g., symmetry) of the building blocks should not be affected by the branching center.<sup>37</sup> Among the different QM methods available nowadays, adiabatic time-dependent density functional theory (TD-DFT) is currently the method of choice for calculating the ES of sizable molecular systems.<sup>48–55</sup> Arbitrary frequency-dependent NLO polarizabilities can be subsequently derived on the basis of the quasi-particle formalism of the TD-Kohn–Sham equations.<sup>56</sup> This method has been applied to calculate OPA and TPA responses of various substituted chromophores.<sup>17,25,26,31,35,37,57–63</sup> These studies have shown the good performances of the TD-DFT-based hybrid functionals for molecular NLO properties.

In this paper, we present a theoretical investigation, mainly based on the above mentioned density matrix formalism of TD-DFT for NLO responses,<sup>17</sup> of two 1,2,3-triazole-based series compiling a total of 19 compounds (Figure 1). The case of **dai**, **dfl**, **2dai**, and **3dfl** has already been analyzed in detail elsewhere,<sup>31</sup> and we recall here the main findings as well as further interpretation for the sake of comparison to other **nd** and **ndi** chromophores. Our purpose is to address two main points: (*i*) the branching effect, which appears to show a quite different behavior than that reported for analogous multibranched chromophores, and (*ii*) the influence of position isomerism on both OPA and TPA responses. To our knowledge, it is the first time that TPA properties have been investigated on four-member branched chromophores<sup>64,65</sup> as well as in relation to regiosomerism. Our findings will also be analyzed in the framework of the Frenkel exciton model. After a brief description of computational details,

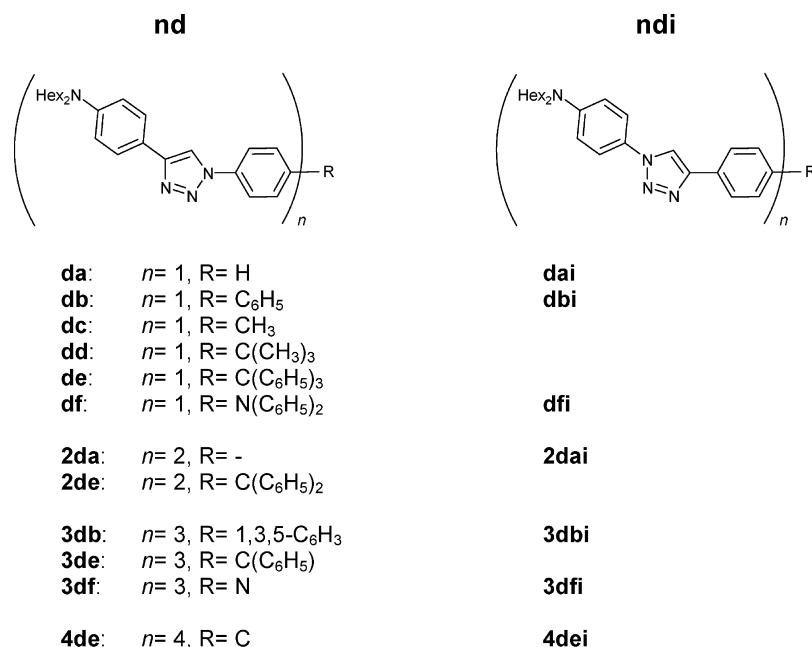


**Figure 1.** Molecular structures of 1,2,3-triazole-based **nd** chromophores (left) and corresponding **ndi** position isomers (right). Hexyl solubilizing chains have been replaced by methyl groups.

already well documented, we will first validate our computational approach for both series of chromophores. This is thought to allow inference with what extent a comparison to experiments is reasonable, i.e., underline all sources of possible discrepancies. After analysis of the main geometrical features, we will sequentially investigate OPA and TPA responses. For both properties, we first analyze trends within each of the two series and subsequently discuss effects of position isomerism. Where appropriate, a comparison to related branched structures will be made. The main findings will be summarized in the concluding section. We believe that this detailed theoretical study performed on a large set of compounds contributes to the overall understanding of structure–properties relationships of NLO chromophores and opens new perspectives for further improvements within the branching strategy.

## II. Computational Methodology

A set of 19 chromophores, sketched in Figure 1, have been theoretically investigated. They are classified in two different series, series **nd** and corresponding 1,2,3-triazole position isomers **ndi**. For the sake of simplicity and reduction of the numerical cost, the hexyl solubilizing chains of original chromophores<sup>4,13,40,41</sup> have been replaced by methyl groups. These two series contain nine dipoles, three quadrupoles, five three-branched chromophores, and two four-branched compounds. All QM calculations have been performed using either Gaussian 98<sup>66</sup> or Gaussian 03 packages<sup>67</sup> in vacuum. For ground state geometries (Figures 2 and S1 and S2, Supporting Information), it was previously found that the Hartree–Fock (HF) method is superior to the DFT-based approaches by reproducing bond length alternation in similar conjugated molecules.<sup>57</sup> It was also shown to be a good compromise for subsequent calculation of optical spectra.<sup>17,25,26,37,57–60,63</sup> Thus, all ground state geometries have

been optimized at the HF/6-31G level of theory, starting from a few different conformations, but no exhaustive sampling has been conducted.

Linear and nonlinear optical responses have been calculated using the density matrix formalism, as described in ref 56. Subsequent computation of TPA cross-sections is detailed in ref 17. We retained the TD-B3LYP/6-31G//HF/6-31G level of theory, in conventional quantum chemical notation “single point//optimization level”, for the calculation of optical spectra, as it was shown to be a good compromise between numerical resources and accuracy and led to quite good agreement with experimental results for a large set of related chromophores. The forthcoming section will be devoted to discussing the validity of such an approach for the present triazole-based chromophores and include a comparison to results obtained with a larger amount of orbital exchange, namely, the hybrid BHandH functional instead of B3LYP. The calculated ES structures include 20, 30, 40, and 60 ESs respectively for dipolar, quadrupolar, three-branched, and four-branched compounds. The number of ESs was checked for at least one dipole, quadrupole, and octupole. It was found to be sufficient as asymptotic values are reached for the absorption spectra, and only small effects (the largest deviation observed is 12% for the first band of **3dbi** when using 24 instead of 40 ESs) are discerned for the amplitude of the TPA spectra.

Besides the number of ESs, a few other parameters influence the calculated response amplitudes. First, the damping factor introduced to simulate finite line width in the resonant spectra has been fixed to 0.20 eV for all chromophores, on the basis of typical broadening seen in available experimental absorption spectra (Table S1, Supporting Information). Next, no solvation effects have been accounted for in the present work. In fact, due to different solute and solvent polarizabilities, the commonly used

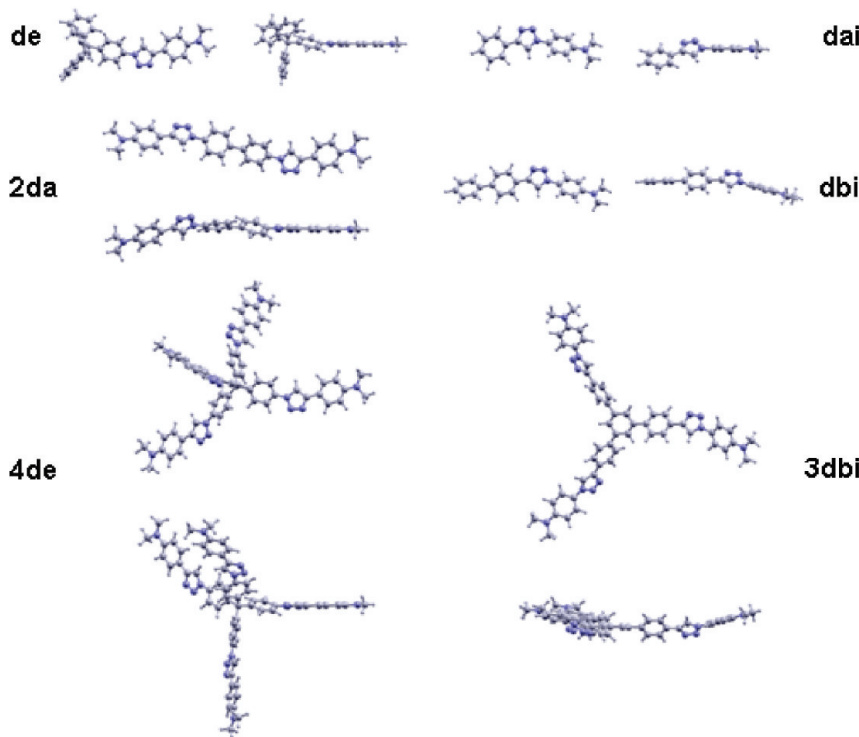


**Figure 2.** Optimized ground state molecular geometries at the HF/6-31G level of theory for selected **nd** (left) and **ndi** (right) chromophores.

**Table 1.** Calculated One-Photon Vertical Absorption Maxima at the TD-B3LYP/6-31G//HF/6-31G Level in Vacuum and Experimental One-Photon Absorption Maxima in Toluene<sup>4,13,40 a</sup>

	<b>2da</b>		<b>3db</b>		<b>dai</b>	<b>dbi</b>	<b>2dai</b>	<b>3dbi</b>	<b>3dfi</b>	<b>4dei</b>
$\lambda^{\text{calcd}}$ nm (eV)	388 (3.19)	280 (4.42)	381 (3.25)	274 (4.52)	286 (4.34)	299 <sup>b</sup> (4.15)	313 <sup>b</sup> (3.96)	303 (4.09)	348 <sup>b</sup> (3.56)	292 (4.25)
$\lambda^{\text{exptl}}$ nm (eV)	350 <sup>c</sup> (3.54)	296 <sup>c</sup> (4.19)	347 <sup>c</sup> (3.57)	293 <sup>c</sup> (4.23)	303 <sup>c</sup> (4.09)	310 <sup>d</sup> (4.00)	325 <sup>d,e</sup> (3.82)	317 <sup>c</sup> (3.91)	347 <sup>e</sup> (3.57)	311 <sup>c</sup> (3.99)

<sup>a</sup> In parentheses, corresponding transition energies in eV. <sup>b</sup> From ref 31. <sup>c</sup> From ref 40. <sup>d</sup> From ref 13. <sup>e</sup> From ref 4.

Lorentz local field factor correction is clearly inappropriate. In addition, relevant treatment of solvent effects is more time-consuming and may lead to further charge transfer overestimation.<sup>17</sup> Last, no vibrational contributions have been considered. All of these effects will influence computed OPA and TPA spectra, and these approximations should always be kept in mind when comparison to experimental findings is sought.

Natural transition orbital (NTO) analysis of the ES<sup>68</sup> has been used to analyze the nature of the ES involved in the photophysical processes of interest. They offer a compact representation of transition densities in terms of their expansion into single-particle transitions. Figures showing molecular geometries and NTOs were obtained with Xcry-SDen.<sup>69</sup> Use of the Frenkel exciton model within the multibranch strategy is already well documented, and the reader may refer to ref 17 for quadrupoles and three-branched chromophores and to ref 43 for three- and four-branched compounds.

### III. Results and Discussion

**Validation of TD-DFT Approach.** First, let us validate the TD-DFT methodology used to determine the optical responses of the chromophores investigated in this work. A

comparison of TD-B3LYP/6-31G//HF/6-31G results with available experimental photophysical data in toluene<sup>4,13</sup> showed that the employed level of theory fits nicely for members of **ndi** series.<sup>31</sup> Further comparison to experimental data<sup>40</sup> for **dai**, **dbi**, and **4dei** leads to a comparable agreement with a calculated first absorption band slightly blue-shifted with respect to the experimental band position (Table 1). Such a good agreement is not observed for members of **nd** series for which the calculated transition energies of the first absorption band are red-shifted by more than 0.3 eV with respect to experimental ones (Table 1). In addition, experimental absorption spectra of **2da** and **3db** show two bands in the 285–400 nm spectral region.<sup>40</sup> For both compounds, the first one shows up near 3.5 eV and has a molar extinction coefficient 2 to 3 times smaller than the strongest absorption band visible near 4.2 eV.<sup>40</sup> Within TD-B3LYP/6-31G//HF/6-31G, both the ratio between oscillator strengths and the band splitting are significantly overestimated (Table 1, Figures 3 and S7 and S8, Supporting Information). Similar deviations have already been reported for a series of related 1,2,3-triazole-based CT regiosomers<sup>6</sup> at TD-B3LYP/6-31G(d)//B3LYP/6-31G(d), for which the agreement of experimental and calculated band positions and amplitude much depends on the attachment points of

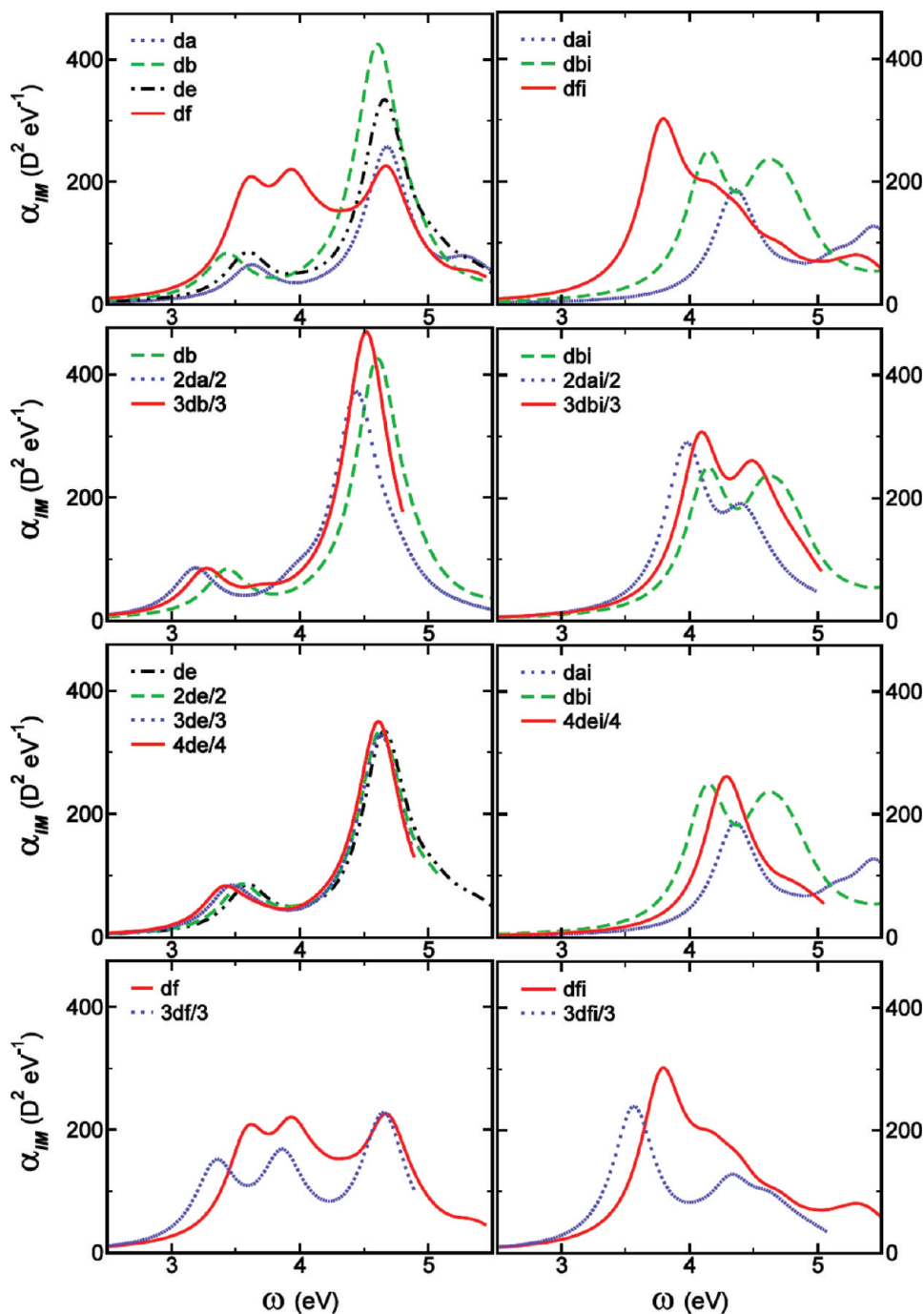


**Figure 3.** Calculated one-photon absorption (OPA) spectra, normalized for the number of branches: **nd** series (left panels), **ndi** series (right panels).

substituents. Here, we may encounter the well-known TD-DFT problem related to an improper description of the excited state with pronounced charge transfer (CT) character. Even hybrid functionals with a moderate amount of orbital exchange such as the B3LYP model are affected by this problem by placing the CT states energetically too low and by miscalculating their optical transition dipoles compared to experimental results.<sup>54</sup> Functionals that contain a larger fraction of Fock-like orbital exchange have been shown to overcome this problem, but at the expense of accuracy for the absolute band positions.<sup>54</sup> Indeed, using the early hybrid BHandH functional (50% of orbital exchange; TD-BHandH/6-31G//HF/6-31G results are available as Supporting Infor-

mation) leads to an overall blue shift of the first absorption band and to a large deviation from the experimental band position (Figures S3, S7, and S8, Supporting Information). At the same time, the splitting between the first two absorption bands becomes comparable to experimental findings, while the ratio of corresponding oscillator strengths becomes close to unity and thus becomes too small (Figure S3, Supporting Information). As a consequence, the correct empirical amount of orbital exchange for given compounds lies somewhere in between B3LYP and BHandH hybrid functionals. In addition, NTOs obtained within these two hybrid schemes, for a larger set of **nd** compounds (Figures S7–S10, Supporting Information), show an overall good

**Table 2.** Average Torsional Angles in Degrees between Phenyl and Triazole Rings

attachment point	da	db	de	df	2da	3db	3df	4de	dai	dbi	dfi	2dai	3dbi	3dfi	4dei
N	31	31	30	34	30	30	33	28	42	42	42	42	42	42	42
C	2	2	3	3	2	2	2	3	1	0	2	3	5	9	7

correspondence, between B3LYP and BHandH results, for the ESs relevant for the main OPA and TPA bands, with a few exceptions. As expected, one observes a somewhat larger delocalization within BHandH, particularly visible on corresponding holes. However, the few exceptions confirm that the optimal fraction of exchange is a system-dependent parameter.<sup>54</sup> Even so, B3LYP results suffer from a certain amount of inaccuracy; we believe that the main trends to be discussed in the present work are trustworthy. For the sake of consistency, we will stick to B3LYP throughout the manuscript, while BHandH results will be given as Supporting Information. We emphasize that a comparison between **nd** and **ndi** series should not concern absolute amplitudes, and all other approximations, namely fixed line width, limited number of ESs, and absence of solvent and vibrational contributions, should always be kept in mind, especially for comparison to experimental data.

**Molecular Geometry.** When experiments are performed in solution at room temperature, various molecular conformations coexist, leading to inhomogeneous broadening of optical spectra. Even if the expected symmetry is not strictly retained, reminiscence of symmetry elements, such as centrosymmetry for quadrupoles<sup>70</sup> or C<sub>3</sub><sup>47</sup> or T<sup>43</sup> symmetry for three- or four-branched chromophores, is still observed in experimental findings and is often very useful in supporting an interpretation. In addition, the amount of possible conformations increases with the number of monomeric units building up the multibranched molecule of interest. For these reasons, we did not perform an exhaustive review of attainable molecular arrangements. For the chromophores studied in the present work, the main conformational degree of freedom concerns torsional angles and the sequence of corresponding signs. Explored geometries showed small energy differences compared to kT at room temperature. End groups may be either approximately coplanar or perpendicular to the molecular mean plane (Figures 2 and S1 and S2, Supporting Information). This may modify the state dipole moment, both in amplitude and vector components. But, it remains small enough to keep all chromophores in the so-called *neutral* class of chromophores experiencing no or little solvatochromic behavior of their absorption spectra.<sup>42,71–73</sup> For **2d** compounds, we retained the conformation closest to inversion symmetry (Figure 2). For **3d** compounds, the central triphenylamine (TPAmine) or triphenylbenzene (TPB) cores allow for either left- or right-handed skewness of the propeller core. Successive twist angles have been selected to ensure C<sub>3</sub> symmetry and approximate planar geometries (Figure 2). The case of **4de** and **nde** chromophores is somewhat more involved. First, chiral tetrahedral symmetry cannot be satisfied due to the geometry of the molecular branches. Among the carbon-cored tetraphenyl analogs reported in the Cambridge Structural Data Base,<sup>74</sup> some have almost D<sub>2</sub> symmetry with phenyls related two-by-two like two butterflies;<sup>75</sup> other have two-by-two almost perpendicular

branches.<sup>76</sup> For the present study, we retained the latter type of conformation (Figure 2), which also approximates tetrahedral symmetry well enough to lead to quasi-degeneracy of the three first ESs.<sup>43</sup>

The ground state optimized geometries of the branched structures show geometrical parameters for each branch quasi-identical to those of their dipolar counterparts. Twist angles around BP, TPAmine, or TPB cores are all of about 45°, in line with those reported for related dipolar,<sup>25,26,29</sup> quadrupolar,<sup>37</sup> and three-branched<sup>25,26,29</sup> chromophores. Despite a reduction of conjugation, as a result of the large twist angles, it has been demonstrated that significant electron communications can still be in action and can lead to enhanced NLO responses.<sup>17</sup> The triazole moiety introduces additional twist angles along the molecular backbone which are significantly larger within **ndi** series than for members of **nd** series, with a larger torsion for the phenyl ring connected to the nitrogen atom of the triazole ring (Table 2). The latter is about 42° for members of **ndi** series, while it is about 30° for compounds of **nd** series. The latter is located in the middle of **nd**'s molecular branches and thus favors electronic decoupling of both molecular ends. This may accentuate the CT problem discussed in the previous section. The twist with the phenyl ring connected to the carbon atom is much smaller, ranging between 1 and 12° (Table 2). These findings are consistent with the structural parameters of related triazole-based structures reported in the Cambridge Structural Data Base.<sup>74</sup>

**One-Photon Absorption (OPA).** **nd** Series. Given the 0.3 eV red shift observed between available experimental data and calculated transition energies (Table 1), all members of **nd** series are predicted to show good transparency in the visible region (Figure 3). The first transition has strong CT character, somewhat overestimated within B3LYP; thus the overlap between electron and hole wave functions is small and results in a small oscillator strength (Figure 3). As visible from the respective NTOs (Figures 4–6 and S7–S12, Supporting Information), the nature of the partial CT is preserved all along the series and corresponds to CT from the triazole–phenyl–NMe<sub>2</sub> end group to the opposite end (core in multibranched systems). As the chemical composition of the latter changes along the series, the transition energy of the first band changes as well. This is not the case for the main contribution to absorption, which is dominated by a (few for multibranched systems) higher lying ES near 4.6 eV for all members of the **nd** series. NTOs illustrate the nice correspondence observed all along the series and the large wave function overlap facilitating the large oscillator strength (Figures 6 and S11, Supporting Information). It should be noticed that for multibranched compounds, the oscillator strength is shared between several ESs, which are not all reported in Figure 4 (**4de**) for the sake of conciseness (Figures S11 and S12, Supporting Information). As both hole

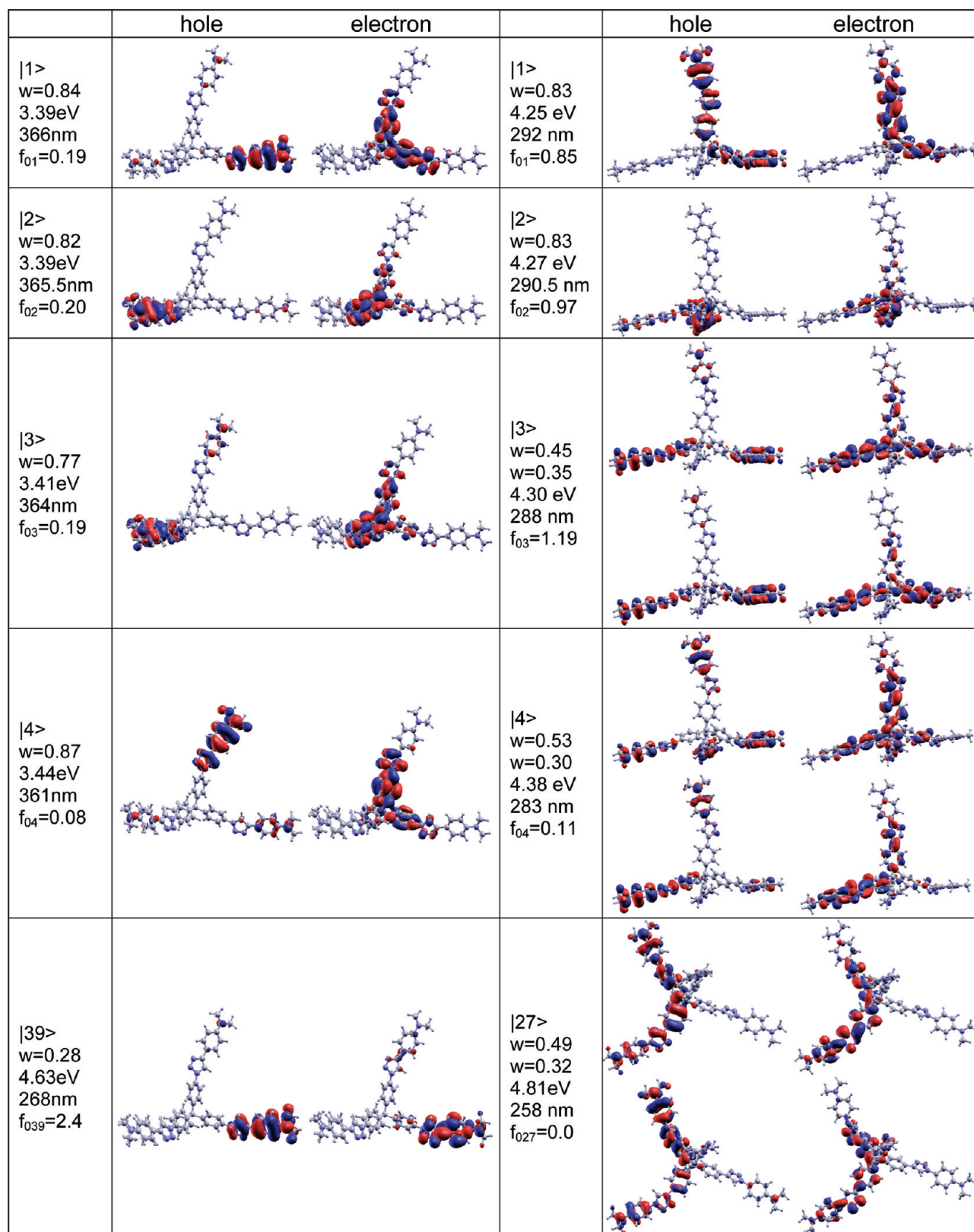


**Figure 4.** Natural transition orbitals<sup>68</sup> of **4de** (left panels) and **4dei** (right panels). Text quote in sequence excited state number, associated eigenvalues, transition energies, transition wavelengths, and oscillator strengths.

and electron are located on the peripheral triazole–phenyl–NMe<sub>2</sub> moiety, it is little influenced by chemical substitution on the other end, by the nature of the core or by interbranch interactions in multimers, and stays around 270 nm over all **nd** series. Thus, transition energies are hardly affected by the other molecular extreme or branching center.

It should be noticed that, in the case of quadrupolar series, a conclusion is less straightforward regarding the nature of the relevant ES bearing the main OPA oscillator strength. Within B3LYP, ES  $|9\rangle$  bears the largest oscillator strength but has both the hole and electron located at the molecular center (Figure S7, Supporting Information), while BHandH

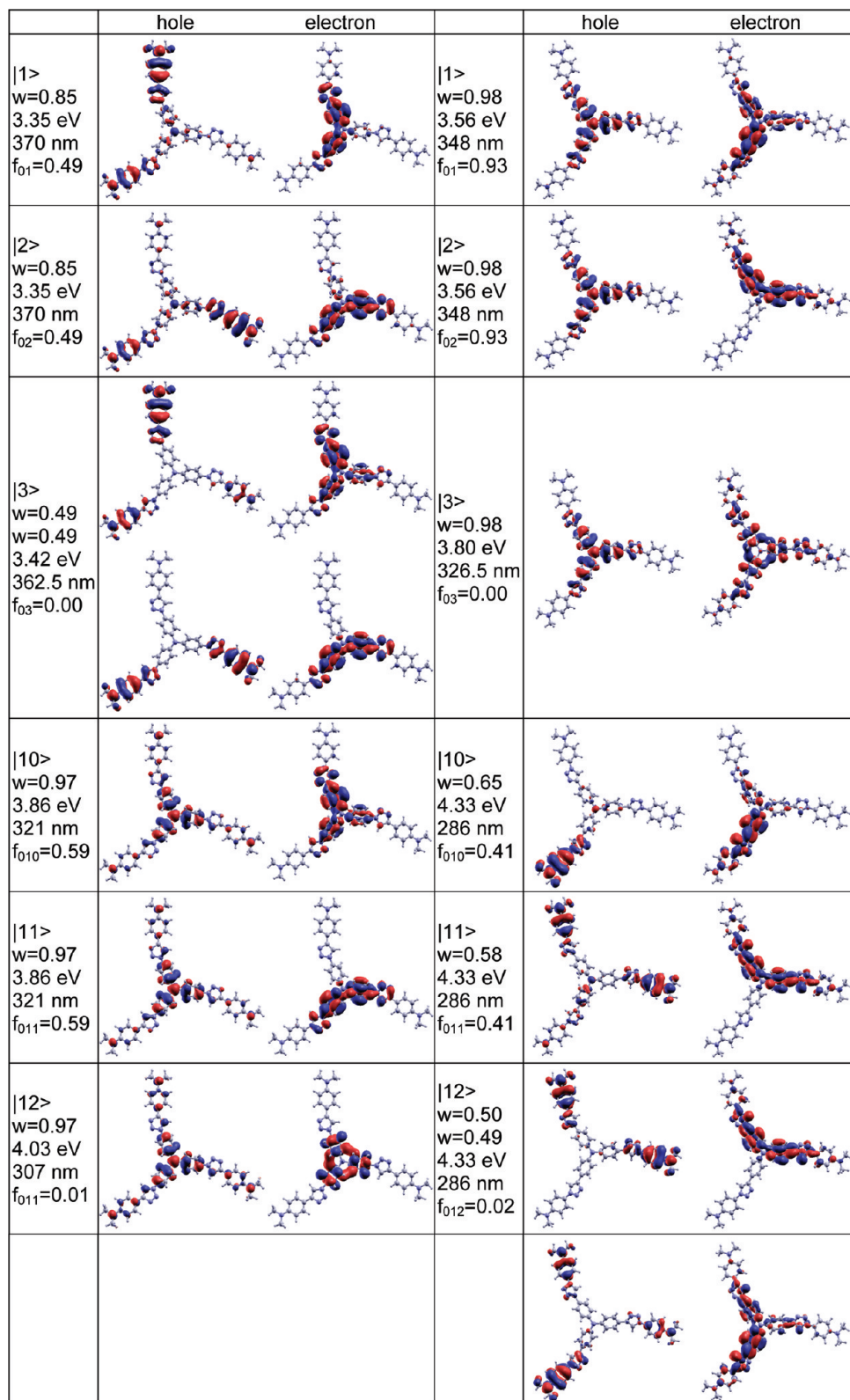


**Figure 5.** Natural transition orbitals<sup>68</sup> of **3df** (left panels) and **3dfi** (right panels). Text quote in sequence excited state number, associated eigenvalues, transition energies, transition wavelengths, and oscillator strengths.

leads to bright state  $|5\rangle$  with major weight on the molecular ends (Figure S7, similar to ESs  $|10\rangle$  and  $|11\rangle$  of **3db** shown Figure S8, Supporting Information), consistent with the above-mentioned picture. Within B3LYP, ES  $|12\rangle$  shows up at 4.68 eV with comparable shape but is a dark state for symmetry reasons, while ES  $|13\rangle$  is a mixture with only a

small amount of oscillator strength (Figure S7, Supporting Information).

In addition, comparison of related dipolar chromophores (**da** with **db** (Figure 3) and **dc** up to **de** (Figure S4, Supporting Information)) shows a slight but systematic red shift and amplitude increase with increasing molecular size. This shows

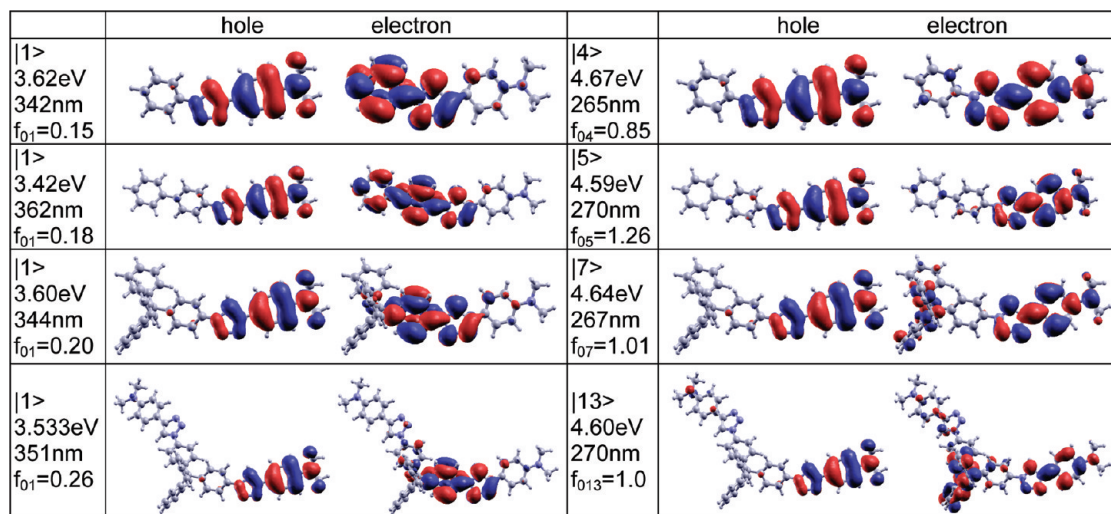


**Figure 6.** Natural transition orbitals<sup>68</sup> relevant for the first (left panels) and main (right panels) one-photon absorption (OPA) band of **da** (top), **db** (middle top), **de** (middle bottom), and **2de** (bottom). Text quote in sequence excited state number, associated transition energies, transition wavelengths, and oscillator strengths.

that the choice for the dipolar unit used to investigate efficiency of the branching strategy may be important. Normalized absorption spectra show an overall additive behavior upon branching with no major enhancement or weakening (Figures 3 and S3, Supporting Information).

**ndi Series.** For all members of this series, the main contribution to the first absorption band arises from the first (first few for multibranched chromophores) ES, which bears significant oscillator strength (Figure 3). Despite the expected red shift upon branching, all chromophores maintain excellent transparency in the visible region. Comparison to the related chromophores<sup>31</sup> shows a systematic blue shift of the first ES but only a slight reduction of the corresponding oscillator strength. This decrease has to be related to the large twist angle introduced by the triazole moiety (Table 2). Close-lying higher ESs bearing significant oscillator strength lead to broad absorption spectra. NTOs illustrate the nature of corresponding electron redistribution upon excitation. Interestingly, while the holes and electrons associated with the first ES of **dai**, **dbi**,<sup>31</sup> **2dai**,<sup>31</sup> **3dbi**, and **4dei** are very similar (Figures 4 and 7 and S13, Supporting Information), with a periphery to core electronic redistribution, those of **dfi**<sup>31</sup> (Figure S9, Supporting Information) and **3dfi**<sup>31</sup> (Figure 5) are much different, as they both involve the TPAmine core up to the triazole moiety. The latter are quite similar to those reported for a three-branched structure built by gathering three quadrupolar chromophores connected via common nitrogen.<sup>37</sup> In both cases, there is a competition between the donating TPAmine core and donating NMe<sub>2</sub> end groups, resulting in a larger donating character for the former. Normalized absorption spectra shown Figure 3 illustrate the different behavior upon branching. Again, to discuss OPA amplitude enhancement, the choice of monomeric analog is crucial, as can be seen from the comparison of **dai** and **dbi** spectra (Figure 3). Using **dbi** as a reference, both **2dai** and **3dbi** show significant enhancement of the first absorption band (Figure 3), due to significant delocalization across the branching cores (Figures 7 and S13, Supporting Information), while that of **4dei** is almost additive. On the contrary, the normalized amplitude of **3dfi** decreases (Figure 3) as a result

of slightly reduced delocalization of both the hole and the electron of its first ES<sup>31</sup> (Figure 5 and S9, Supporting Information).

**Position Isomerism.** A comparison between members of **nd** and **ndi** series shows quite a few dramatic changes directly related to position isomerism of the 1,2,3-triazole ring. Due to the inverted position of the triazole ring, compounds of **nd** series have a large twist angle in the middle of the molecular backbone which potentially may disrupt their electronic communication between both molecular ends (Figures 2 and S1 and S2, Supporting Information; Table 2). As a consequence, NTOs associated with the first excited state are less delocalized over the molecular backbone and corresponding oscillator strength are smaller than what is observed within **ndi** series (Figures 4 and 5). While for all **ndi** members the first ES contributes predominantly to the main absorption band, **nd** compounds have a first absorption band with reduced amplitude followed by a stronger band showing up at approximately the same position for all members of the series (Figure 3).

Further comparison requires splitting both series into two subassemblies. Let us first concentrate on chromophores that do not contain the TPAmine moiety. For all of them, the terminal NMe<sub>2</sub> group acts as the donating unit while the opposite core or end group, which may extend up to the triazole moiety, has electron-withdrawing character. For these compounds, one observes a systematic red shift for **nd** members as compared to the **ndi** analogs, but all maintain transparency in the visible region (Figure 3). The situation is quite different for the TPAmine-based chromophores as the donating characters of the different amino groups compete. First, despite the two donating end groups, neither **df** nor **dfi** can be assimilated to a quadrupole (Figure S9, Supporting Information). In fact, the branches deviate significantly from quadrupoles, as both the chemical difference between TPamine and NMe<sub>2</sub> and the dissymmetry of the 1,2,3-triazole moiety significantly break molecular symmetry. A comparison of NTOs of **df** and **3df** with those of **dfi** (Figure S9, Supporting Information) and **3dfi** (Figure 5), respectively, shows a nice correspondence and nicely

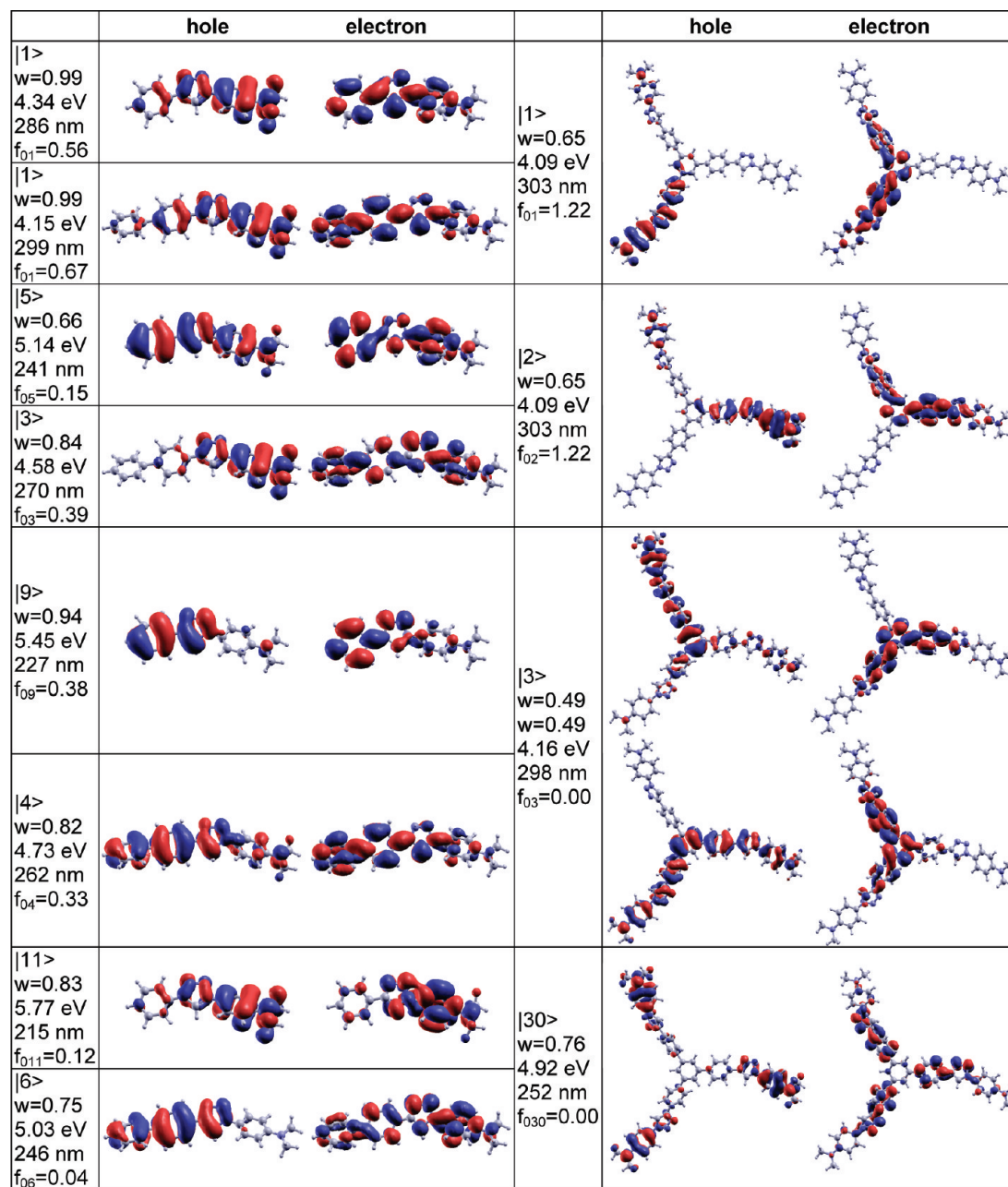


**Figure 7.** Natural transition orbitals<sup>68</sup> of **dai** (left panels, first line), **dbi** (left panels, second line), and **3dbi** (right panels). Text quote in sequence excited state number, associated eigenvalues, transition energies, transition wavelengths, and oscillator strengths.

illustrates the competition between the donating moieties. Indeed, one observes a clear correspondence between the ES  $|1\rangle$  ( $|3\rangle$ ) of **df** with the ES  $|6\rangle$  ( $|1\rangle$ ) of **dfi**. The same holds when ESs  $|1\rangle$  and  $|2\rangle$  ( $|10\rangle$  and  $|11\rangle$ ) of **3df** are compared to the  $|10\rangle$  and  $|11\rangle$  ( $|1\rangle$  and  $|2\rangle$ ) of **3dfi**. The slight differences especially visible on the triazole moiety are directly related to the amplitude of the torsional angles with neighboring phenyl rings. Given the CT problem encountered for **ndf** members, the small residual differences with **ndfi** transition energies after a systematic blue shift of **ndf** ones does not allow for a conclusion about the sign of the shift induced by position isomerism.

We underline that none of these NTOs evidence a strong participation of the triazole ring as electron donating or withdrawing species, when compared to all other moieties building the chromophores. Its main effect is to allow for a

significant blue shift as compared to related dipolar,<sup>25,26,29</sup> quadrupolar,<sup>70</sup> and three-branched<sup>26,27,34,37,77</sup> chromophores and triggers the competition between similar end groups while maintaining good OPA responses. These findings corroborate with what has been previously inferred for isomeric triazole-based CT chromophores<sup>6</sup> and for hyperbranched poly(1,2,3-triazole)'s.<sup>7</sup> In fact, Tang et al.<sup>7</sup> conclude that “there exist ground-state interaction between TPAmine and triazole moieties in the polymers and that the electronic communications are dictated by the regioisomeric structures”, and Diederich et al.<sup>6</sup> state that “1,2,3-triazole makes a particularly intriguing linker where the CT path is interrupted... CT can occur and may be even quite efficient depending on the substitution pattern... responsible for about

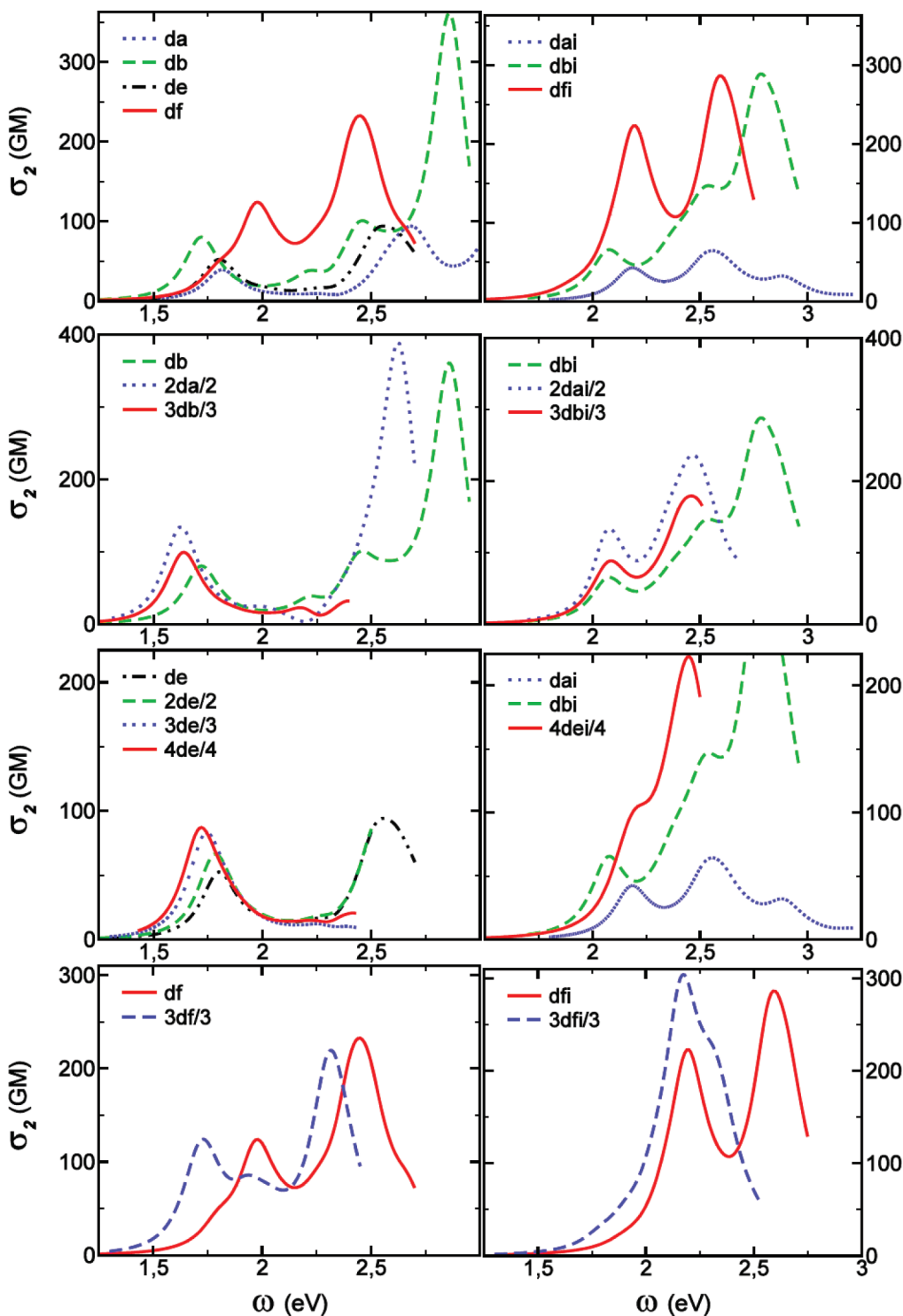


**Figure 8.** Calculated two-photon absorption (TPA) spectra, normalized for the number of branches: **nd** series (Left panels), **ndi** series (right panels).

50 nm range of transition energies and also affects strongly the absorption intensities”.

Finally, despite the expected red shift upon branching, all chromophores investigated in the present work maintain excellent transparency in the visible region. These findings corroborate experimental data<sup>4,13,40,41</sup> and confirm that these triazole-based chromophores are good candidates for optical limiting in the visible region.<sup>4</sup>

**Two-Photon Absorption (TPA). *nd* Series.** Given that our results for this series may be affected by the CT problem

discussed above, let us first determine to what extent an analysis of TPA properties is reasonable at the B3LYP level of theory. Comparison to BH&H calculations shows that the ES at the origin of the first TPA band keeps the same number, and corresponding NTOs have similar shapes (Figures S7–S10, Supporting Information) except for **df**. In both types of calculations, higher lying ESs are responsible for the appearance of additional TPA bands having larger TPA amplitudes (Figures 8 and S5 and S6, Supporting Information). The behavior upon branching regarding am-

plitudes is also consistent within the two levels of theories (Figures 8 and S5, Supporting Information). The main difference concerns transition energies and especially state splitting, which prevents any inference about the strength of the interbranch coupling within the Frenkel excitonic scheme. Indeed, B3LYP would lead to coupling energies less than 0.02 eV, while BHandH gives up to 0.09 eV for **3df** (Figures S7–S10, Supporting Information).

For all but **df**, the first TPA maximum is found where expected, i.e., at the energy of the first, second, third, and fourth ES respectively for all other dipoles, two-branched, three-branched, and four-branched compounds. This is consistent with the Frenkel excitonic picture where dipolar species are approximated by a single ES. The corresponding electronic redistribution involves a periphery NMe<sub>2</sub> to core electronic redistribution (Figures 4, 5, and 7 and S7 and S8, Supporting Information). Interestingly, **df** has only a weak shoulder near the first ES, while the main contribution to the first TPA band arises from the third ES (Figures 8 and S5 and S9, Supporting Information). This may be a consequence of a pseudoquadrupolar behavior of **df**, which bears nitrogen-based end groups that compete. Further inference about the underlying electronic redistribution of relevant ESs is hindered by significant differences between NTOs obtained at the B3LYP and BHandH levels of theory (Figure S9, Supporting Information). The case of **3df** is less tricky (Figure 5) thanks to the additional dissymmetry introduced on the TPAmine core, which is trifunctionalized in the multimer, in a similar way to what has been obtained for an analogous branched chromophore built by gathering three quadrupolar units through a TPamine core.<sup>37</sup> Even larger TPA amplitudes are predicted at higher energies (Figures 8 and S5) for all but **3db**, **3de**, and **4de**, for which analysis is limited by the number of ESs accounted for in our calculations. Unfortunately, a systematic interrelationship with given ESs is difficult, and no general feature emerges from an inspection of NTOs that have been identified (Figures S9 and S10, Supporting Information).

In the investigation of branching strategy, it is worthwhile to emphasize the crucial role played by the choice of the benchmark monomer. Whereas only slight variations of both amplitudes and band position occur for various substitution of the sp<sup>3</sup> carbon branching center (going from **dc** to **de**, Figure S6, Supporting Information), the differences are large when replacing the phenyl end group of **da** with a BP moiety to build **db** (Figure 8). The BP moiety not only stabilizes the first ES but also leads to a 2-fold increase of the corresponding TPA amplitude thanks to an expansion of delocalization over the BP end group (Figure 6).

Whereas an overall additive behavior was observed for OPA, the branching strategy is shown to be efficient for TPA responses (Figure 8). Once more, the TPAmine-based chromophores are the exceptions among the series, as the amplitude of the main TPA bands reveals essentially an additive behavior. Enhancement and reduction in a specific spectral region are also observed. The overall behavior is quite similar to what has been reported for a branched quadrupole,<sup>37</sup> but careful inspection of the relevant NTOs shows that the nature of the ES in question is much less

modified by the branching center. There is a clear correspondence between ES |1⟩ of **df** (Figure S9, Supporting Information) and |3⟩ of **3df** (Figure 5). Within this picture, the amplitude of the first TPA band of **3df** has to be compared to the shoulder near 1.8 eV in the TPA spectra of **df**, and we recover the large enhancement expected for TPAmine branched dipoles.<sup>25,26</sup> Despite similarities between the NTO of |3⟩ of **df** (Figure S9, Supporting Information) and |27⟩ of **3df** (Figure 5), the large blue shift of the latter prompts care in further interpretation. On the contrary, the picture is simple for all other members of this series, as the first TPA band of monomers can be safely attributed to ES |1⟩ and that of multimers to what predicts the exciton model. The quadrupole **2da** shows the largest enhancement (a factor of 2 with respect to **db**) thanks to through-BP-core communication (Figures 8 and S7, Supporting Information). **3db** evidences much less enhancement consistently with the other TPBcore<sup>17</sup> analogs for which functionalization in meta-positions inhibits interbranch conjugation (Figures 8 and S8, Supporting Information). It should be noticed that comparison to the benchmark chromophore bearing a TPB end group instead of BP would most probably lead at best to additive and, at worst, to reduced TPA responses.<sup>29</sup> The case of C-centered branched chromophores is quite surprising, as little through-bond cross-talk is expected. Surprisingly, we observe a large enhancement that increases with an increasing number of branches from **2de** up to **4de** (Figure 8). Unfortunately, without any reasonable estimate for the interbranch coupling, it is hard to conclude about the underlying nature of the interbranch interactions that may be mainly electrostatic or involve coherent interbranch interaction.

**ndi Series.** Let us start with the monomeric benchmark chromophores. For the sake of conciseness, we did not consider any of the monomers substituted by sp<sup>3</sup> carbons. Results obtained on **nd** series reveal only slight modifications between **da** and sp<sup>3</sup> carbon analogs, the latter having properties in between those of **da** and **db** (Figure 8). Thus, **dai** and **dbi** will respectively be used as lower and upper limits for investigating the effect of branching in all branched chromophores missing TPAmine. Figure 8 reports calculated TPA spectra for the three monomers **dai**, **dbi**, and **dfi**. Replacement of the phenyl end group by either BP or TPAmine leads to a dramatic increase of the TPA response, with the same trends previously observed for the respective OPA (Figure 3). These substitutions induce respectively significant red and slight blue shifts of the first TPA band. The latter is quite surprising given the large red shift observed for the main OPA band (Figure 3). In fact, the first TPA band of both **dai** and **dbi** mainly involves ES |1⟩, which also dominates the OPA spectra. On the contrary, that of **dfi** originates from ES |6⟩ (Figure 8 and S9, Supporting Information), while ES |1⟩ appears as a very slight shoulder on the low-energy part of the spectrum. A comparison of corresponding NTOs is informative, as ES |6⟩ of **dfi** (Figure S9, Supporting Information) shows a similar periphery to core electronic redistribution to ES |1⟩ of **dai** and **dbi** (Figure 7). Thus, while for the first OPA band, the nature of the underlying electronic redistribution is completely different

for **d<sub>fi</sub>**, it is not for the final TPA state, giving rise to the first TPA band. Furthermore, the NTO of an electron for **d<sub>fi</sub>** is the same for ES |1⟩ and ES |6⟩, while the respective hole orbitals involve either TPAmine or NMe<sub>2</sub> end groups, indicating the competition between the two donating nitrogen-based moieties (Figure S9, Supporting Information). The second TPA maxima near 2.5 eV (Figure 8) can be assigned to ESs |5⟩, |6⟩, and |13⟩ respectively for **dai**, **dbi** (Figure 7), and **d<sub>fi</sub>** (Figure S9, Supporting Information).

TPA spectra normalized for the number of branches, reported in Figure 8, reveal significant enhancement for all branched chromophores with coincident peak positions (shoulder for **4dei**) for the first TPA band. Higher-lying ESs lead to even larger TPA responses on the high-energy part of the spectra (Figures 4 and 7), except for **3dfi**, for which analysis is hindered by the limited number of ESs accounted for. For all branched chromophores but **3dfi**, the first TPA maximum is found consistently with the Frenkel exciton model predictions: the second, third, and fourth ES for **2dai**, **3dbi**, and **4dei**, respectively. The final ES involves a periphery (NMe<sub>2</sub>) to core electronic redistribution (Figures 4 and 6 and S13, Supporting Information) that nicely compares with ES |1⟩ of **dai** and **dbi** (Figure 7), especially for **3dbi** and **4dei**. However, predicted state splitting with respect to benchmark monomers is not at all satisfied and manifests itself by correspondence in band position of the first TPA bands of monomers and multimers. From the state splitting calculated for each multimer, estimates of the interbranch coupling lead to 0.02, 0.03, and 0.08 eV for **3dbi**, **4dei**, and both **2dai** and **3dfi**, respectively. These findings correlate nicely with the shapes of corresponding NTOs as the hole and electrons have at least significant if not prevailing weight on the branching center for the last two chromophores. **3dbi** evidences the lowest enhancement among the series, as was the case for **3db**, and the same reasoning holds. The case of C-centered branched chromophores **4dei** is similar to that of **3dbi**, as the enhancement near 2.2 eV partly results from the tail of the band located near 2.4 eV. The latter can be assigned to a couple of higher-lying excited states such as ES |27⟩ (Figure 4) showing similitude to some degree with ESs |5⟩ and |6⟩ of **dai** and **dbi**, respectively (Figure 7). For **2dai**, the strong through-bond communication allowed by the BP core leads to a significant mixture of dipolar ESs (Figure S13, Supporting Information) and 2-fold enhancement of the normalized TPA amplitude at the first maximum as compared to **dbi**.<sup>31</sup> Contrary to the three other branched **ndi** compounds, but consistent with what has been observed for the benchmark chromophore **d<sub>fi</sub>**, no TPA maximum is visible in the vicinity of ES |3⟩ of **3dfi** (Figures 5 and 8). The main TPA band has to be related to ES |12⟩, and the corresponding NTOs show a marked correspondence with those of ES |6⟩ of **d<sub>fi</sub>**<sup>31</sup> (Figures 8 and S9, Supporting Information). Thus, for all **ndi** chromophores, the first TPA band corresponds to an ES with quasi-identical holes and electrons, i.e., underlying electronic redistribution from the periphery (NMe<sub>2</sub> side) to the core. Moreover, significant enhancement of the normalized TPA amplitude is also in action for **3dfi**. Therefore, the branching strategy is shown to be efficient for all four

investigated cores. The main change occurring for TPAmine-based chromophores is the decoupling of OPA and TPA states, leading to a consequent blue shift of the first TPA maximum, which shows the largest values among both monomers and multimers. Among the reasons for large TPA amplitudes, we notice that higher-lying ESs open the possibility of manifold coupling to the intermediate lower-lying ESs which have sizable transition dipole moments.

**Position Isomerism.** The overall effects of position isomerism of the 1,2,3-triazole ring on TPA responses are less dramatic than those reported for OPA responses, except for TPAmine-based chromophores. In fact, ESs at the origin of the main OPA band are quite different for the two series, but this is not the case for the first TPA band. Consistently with the Frenkel exciton picture, where monomers are reduced to a single ES (being the first ES), large TPA responses originate from the first, second, third, and fourth ESs, respectively, for monomers and two-, three-, and four-branched compounds, for both position isomers. In addition, NTOs of the final ES show comparable periphery (NMe<sub>2</sub> end groups) to core electron redistribution for all. Overall, their delocalization over the molecular branches is significantly larger for **ndi** than for **nd**; even so, comparison is limited due to the occurrence of CT problems for **nd** compounds. Accordingly, transition dipole moments are significantly enhanced for **ndi** chromophores with respect to their **nd** analogs and so are the related TPA responses.

The ranking of TPA amplitudes and relative peak positions among the dipoles stays the same for both position isomers. Substitution of the phenyl ring by a BP moiety leads to a noteworthy increase of TPA amplitudes and red shifts. Further substitution by the TPamine core leads to an additional TPA enhancement but with a significant red shift of the first TPA band.

Interestingly, none of the investigated branched chromophores showed any quantitative agreement with the Frenkel exciton model such as band splitting around the first ES of the benchmark monomer. TPA spectra of **nd** chromophores undergo significant red shifts with respect to their monomeric counterpart, while the first TPA maximum of each **ndi** chromophore shows up almost at the same energy as its dipolar benchmark. On the contrary, the behavior upon branching is quite similar in both series with moderate enhancement for the TPB core, sizable enhancement for the sp<sup>3</sup> carbon core, and a 2-fold increase for the BP core. Thus, combining the branching strategy with inversion of the triazole moiety allows for a spectral tuning of TPA responses to a larger extent than OPA responses, while maintaining the efficiency of cooperative effects.

The different behavior upon triazole inversion in TPamine-based chromophores is directly related to the presence of two donating units instead of one. As already mentioned for investigation of their OPA responses, the triazole moiety controls competition between the two amino groups. This is nicely illustrated by NTOs of relevant ESs. Indeed, there is a clear correspondence between NTOs of ESs |3⟩ of **3df** and |12⟩ of **3dfi** (Figure 5). These final ESs contribute predominantly to the first TPA band. They involve periphery to core electronic redistribution comparable to what was found for

the compounds missing the TPAmine moiety. The same conclusions hold for ESs |1⟩ of **df** and |6⟩ of **dfl** (Figure S9, Supporting Information). Moreover, NTOs of ESs |12⟩ of **3df** and |3⟩ of **3dfl** (Figure 5) also have very similar shapes and are thus consistent with the picture of competing end groups. Because corresponding electronic redistributions are localized on the molecular center, they do not contribute strongly to the TPA responses. Thus, the overall competition between the donating end groups explains why both **dfl** and **3dfl** have their first TPA maximum far blue-shifted from the position expected from simple reasoning.

#### IV. Conclusion

In conclusion, our quantum-chemical study based on TD-DFT methodology reveals that the introduction of triazole leads to dramatic changes in optical properties of chromophores especially for multibranched systems. The triazole ring substantially modifies electronic communication and delocalization between the electron donating end groups and the branching center via torsion between phenyl and triazole rings (which modifies  $\pi$  conjugation) as well as through its position isomerism. This adds to the multibranching interactions allowing for stark and intuitively unexpected modifications of the excited state structure and, subsequently, relevant linear and nonlinear optical responses. In particular, when compared to the related analogs, introduction of the triazole moiety in the molecular backbone allows for an overall blue shift of both OPA and TPA bands with a moderate reduction of their response amplitudes. Their ability to be promising candidates for optical limiting in the visible region<sup>4,13</sup> is thus confirmed for a diversified set of chromophores. In addition, larger TPA responses are predicted at higher energies due to contribution from high-lying ESs, as has been found for similar chromophores.<sup>37</sup>

The changes observed between the two investigated 1,2,3-triazole regioisomers can be related to differences in the amplitude of the torsional angles with neighboring phenyl rings. The twist angle with the phenyl substituted at the nitrogen position is significantly larger than that of phenyl attached to the carbon atom. The former is located in the middle of **nd**'s molecular branch(es), thus favoring electronic decoupling of both molecular ends. Besides the overall blue shift when going from **nd** series to **ndi**, this electronic decoupling increases the CT character of the first absorption band and consequently decreases its OPA oscillator strength. The main absorption band shows up near 4.6 eV independently of the **nd** chromophore of interest. This is a direct consequence of hole and electron localization on the peripheral NMe<sub>2</sub> donating moiety that ensures little influence on the relevant ES(s) of chemical substitution on the other end, including the nature of the core or interbranch interactions in multimers. Position isomerism has less impact on TPA properties except for TPAmine-based chromophores. The latter bear nitrogen-based donating moieties on both molecular ends or in the periphery and core for monomers and three-branched derivatives, respectively. Thus, monomers could be thought of as pseudoquadrupoles, but a detailed inspection of NTOs reveals more subtle behavior. In fact, the respective role of TPAmine and NMe<sub>2</sub> moieties is

interchanged and triggered by the triazole moiety. Calculations show that the nature of the electronic redistribution (periphery to TPAmine core) associated with the first TPA band of the three-branched compounds is preserved. As a consequence, while the main contribution to this TPA band arises from the third ES for **3df**, it corresponds to the 12's ES for **3dfl**. In addition, none of the monomers has its first TPA band in the vicinity of the first ES. Thus, the apparent behavior upon branching is dramatically different for both isomers with a large red shift and almost additive behavior for **3df** as compared to **df** and concomitance and enhancement for **3dfl** as compared to **dfl**. This intricate finding renders the Frenkel exciton model useless for these TPAmine-based chromophores.

For all other chromophores, results are qualitatively consistent with the Frenkel exciton picture, as the main TPA band can be associated with the first, second, third, and fourth ESs respectively for dipoles, quadrupoles, and three- and four-branched derivatives. As found for related chromophores, the donating end groups confer an electron-withdrawing character to the BP,<sup>37</sup> TPB,<sup>29</sup> and sp<sup>3</sup> carbon moieties, and monomers have significant dipolar character. The branching strategy is shown to be efficient, as a sizable enhancement of TPA responses are observed with moderate effect for the TPB core and an about 2-fold enhancement for both the BP core and carbon-cored tetramers. However, we underline that the amount of enhancement strongly depends on the choice of the benchmark monomer. In addition, for large chromophores, the increasing number of conformational degrees of freedom may lead to experimentally broadened and reduced TPA responses when performed in solutions at room temperature, as a result of oscillator strength redistribution (intramonomer) and inhomogeneous broadening.

These results and further inspection of NTOs clearly show that the 1,2,3-triazole moiety has neither electron-donating nor an electron-withdrawing character. This corroborates earlier findings where triazole has been described as an intriguing linker that introduces conjugation disruption while maintaining significant electronic communication and optical properties dictated by the regiosiomiceric structure. This subtle acting of the triazole moiety may be combined with complementary routes of molecular engineering. Replacement of donating end groups by electron-withdrawing ones should lead to further blue shifts that may allow keeping full transparency in the visible region for even larger branched systems.<sup>25,26,29</sup> Substitution of the BP core by a fluorene core should allow for increased conjugation along the quadrupolar backbone, and both improve OPA and TPA responses.<sup>37</sup> Slight dissymmetrical functionalization could also offer interesting perspectives for spatial control of the fluorescence properties while maintaining sizable TPA responses.<sup>63</sup>

From the theoretical perspective, these series are also a kind of tutorial example of isomeric compounds that are quite sensitive to the specific exchange-correlation DFT functional in use. In fact, while the description of one of the isomers shows very good agreement with experimental results, e.g., for transition energies and oscillator strength, the other is quite poorly described with the very same functional. In fact, besides comparison to available experimental data, in the

B3LYP model, the first ESs of **nd** members have small integral overlap between their electron and hole orbitals, which renders these states to be optically weak. This small overlap between NTO orbitals of ES indicates its CT nature (in a general sense) and points to a possible overestimated red shift of the transition energy in semilocal DFT models. Nevertheless, an increase of the amount of exact exchange (going from B3LYP to BHandH) allows for at least qualitative interpretation of the optical responses of the studied chromophores. The present example illustrates the need for further improvements in developing a better XC functional, as it shows that an increased amount of exact exchange improves respective oscillator strengths of different electronic transitions, while at the same time the respective transition energies become overestimated.

**Acknowledgment.** We wish to thank Dr. Olivier Mongin and Manuel Parent for stimulating discussions. This work was performed in part at the U.S. Department of Energy, Center for Integrated Nanotechnologies (CINT), at Los Alamos National Laboratory (LANL; contract DE-AC52-06NA25396). This work was granted access to the HPC resources of CINES under the allocation 2005-[c20050822414] and 2008-[x20080825087] made by GENCI (Grand Equipement National de Calcul Intensif).

**Supporting Information Available:** Table of spectral linewidths; additional calculated OPA and TPA spectra; and additional calculated NTOs and corresponding transition energies, transition wavelengths, and oscillator strengths. This material is available free of charge via the Internet at <http://pubs.acs.org>.

## References

- (1) Kolb, H. C.; Finn, M. G.; Sharpless, K. B. Click Chemistry: Diverse Chemical Function from a Few Good Reactions. *Angew. Chem., Int. Ed. Engl.* **2001**, *40*, 2004.
- (2) Qin, A.; Lam, J. W. Y.; Tang, B. Z. Click polymerization. *Chem. Rev.* **2010**, *39*, 2522.
- (3) Zhou, Z.; Fahrni, C. J. A Fluorogenic Probe for the Copper(I)-Catalyzed Azide-Alkyne Ligation Reaction: Modulation of the Fluorescence Emission via  $3(n,\pi^*)$ - $1(\pi,\pi^*)$  Inversion. *J. Am. Chem. Soc.* **2004**, *126*, 8862.
- (4) Parent, M.; Mongin, O.; Kamada, K.; Katan, C.; Blanchard-Desce, M. New chromophores from click chemistry for two-photon absorption and tuneable photoluminescence. *Chem. Commun.* **2005**, 2029.
- (5) Qin, A.; Jim, C. K. W.; Lu, W.; Lam, J. W. Y.; Häussler, M.; Dong, Y.; Sung, H. H. Y.; Williams, I. D.; Wong, G. K. L.; Tang, B. Z. Click Polymerization: Facile Synthesis of Functional Poly(aryltriazole)s by Metal-Free, Regioselective 1,3-Dipolar Cycloaddition. *Macromolecules* **2007**, *40*, 2308.
- (6) Jarowski, P. D.; Wu, Y.-L.; Schweizer, W. B.; Diederich, F. 1,2,3-Triazoles as Conjugative  $\pi$ -Linkers in Push-Pull Chromophores: Importance of Substituent Positioning on Intramolecular Charge-Transfer. *Org. Lett.* **2008**, *10*, 3347.
- (7) Qin, A.; Lam, J. W. Y.; Jim, C. K. W.; Zhang, L.; Yan, J.; Häussler, M.; Liu, J.; Dong, Y.; Liang, D.; Chen, E.; Jia, G.; Tang, B. Z. Hyperbranched polytriazoles: Click polymerization, regiosomeric structure, light emission, and fluorescent patterning. *Macromolecules* **2008**, *41*, 3808.
- (8) Meudtner, Robert, M.; Ostermeier, M.; Goddard, R.; Limberg, C.; Hecht, S. Multifunctional Clickates as Versatile Extended Heteroaromatic Building Blocks: Efficient Synthesis via Click Chemistry, Conformational Preferences, and Metal Coordination. *Chem.—Eur. J.* **2007**, *13*, 9834.
- (9) Schweinfurth, D.; Hardcastle, K. I.; Bunz, U. H. F. 1,3-Dipolar cycloaddition of alkynes to azides. Construction of operationally functional metal responsive fluorophores. *Chem. Commun.* **2008**, 2203.
- (10) Li, Z. a.; Yu, G.; Wu, W.; Liu, Y.; Ye, C.; Qin, J.; Li, Z. Nonlinear Optical Dendrimers from Click Chemistry: Convenient Synthesis, New Function of the Formed Triazole Rings, and Enhanced NLO Effects. *Macromolecules* **2009**, *42*, 3864.
- (11) Li, Z. a.; Yu, G.; Hu, P.; Ye, C.; Liu, Y.; Qin, J.; Li, Z. New Azo-Chromophore-Containing Hyperbranched Polytriazoles Derived from AB<sub>2</sub>Monomers via Click Chemistry under Copper(I) Catalysis. *Macromolecules* **2009**, *42*, 1589.
- (12) Xie, J.; Hu, L.; Shi, W.; Deng, X.; Cao, Z.; Shen, Q. Synthesis and nonlinear optical properties of hyperbranched polytriazole containing second-order nonlinear optical chromophore. *J. Polym. Sci., Part B: Polym. Phys.* **2008**, *46*, 1140.
- (13) Zoon, P. D.; Stokkum, I. H. M. v.; Parent, M.; Mongin, O.; Blanchard-Desce, M.; Brouwer, A. M. Fast photo-processes in triazole-based push-pull systems. *Phys. Chem. Chem. Phys.* **2010**, *12*, 2706.
- (14) Fréchet, J. M. J. Dendrimers and supramolecular chemistry. *Proc. Natl. Acad. Sci. U.S.A.* **2002**, *99*, 4782.
- (15) Sullivan, P. A.; Rommel, H.; Liao, Y.; Olbricht, B. C.; Akelaitis, A. J. P.; Firestone, K. A.; Kang, J.-W.; Luo, J.; Davies, J. A.; Choi, D. H.; Eichinger, B. E.; Reid, P. J.; Chen, A.; Jen, A. K. Y.; Robinson, B. H.; Dalton, L. R. Theory-guided design and synthesis of multichromophore dendrimers: An analysis of the electro-optic effect. *J. Am. Chem. Soc.* **2007**, *129*, 7523.
- (16) He, G. S.; Tan, L. S.; Zheng, Q.; Prasad, P. N. Multiphoton absorbing materials: Molecular designs, characterizations, and applications. *Chem. Rev.* **2008**, *108*, 1245.
- (17) Terenziani, F.; Katan, C.; Badaeva, E.; Tretiak, S.; Blanchard-Desce, M. Enhanced Two-Photon Absorption of Organic Chromophores: Theoretical and Experimental Assessments. *Adv. Mater.* **2008**, *20*, 4641.
- (18) Rumi, M.; Barlow, S.; Wang, J.; Perry, J. W.; Marder, S. R. Two-Photon Absorbing Materials and Two-Photon-Induced Chemistry. In *Photoresponsive Polymers I; Advances in Polymer Science*; Springer-Verlag: Berlin, 2008; Vol. 213, pp 1–95.
- (19) Pawlicki, M.; Collins, H. A.; Denning, R. G.; Anderson, H. L. Two-Photon Absorption and the Design of Two-Photon Dyes. *Angew. Chem., Int. Ed. Engl.* **2009**, *48*, 3244.
- (20) Specht, A.; Bolze, F.; Omran, Z.; Nicoud, J.-F.; Goeldner, M. Photochemical tools to study dynamic biological processes. *HFSP J.* **2009**, *3*, 255.
- (21) Kim, H. M.; Cho, B. R. Two-photon materials with large two-photon cross sections. Structure-property relationship. *Chem. Commun.* **2009**, 153.
- (22) Joshi, M. P.; Swiatkiewicz, J.; Xu, F. M.; Prasad, P. N. Energy transfer coupling of two-photon absorption and reverse

- saturable absorption for enhanced optical power limiting. *Opt. Lett.* **1998**, *23*, 1742.
- (23) Chung, S. J.; Kim, K. S.; Lin, T. H.; He, G. S.; Swiatkiewicz, J.; Prasad, P. N. Cooperative enhancement of two-photon absorption in multi-branched structures. *J. Phys. Chem. B* **1999**, *103*, 10741.
- (24) Cho, B. R.; Son, K. H.; Lee, S. H.; Song, Y. S.; Lee, Y. K.; Jeon, S. J.; Choi, J. H.; Lee, H.; Cho, M. H. Two Photon Absorption Properties of 1,3,5-Tricyano-2,4,6-tris(styryl)benzene Derivatives. *J. Am. Chem. Soc.* **2001**, *123*, 10039.
- (25) Katan, C.; Terenziani, F.; Mongin, O.; Werts, M. H. V.; Porres, L.; Pons, T.; Mertz, J.; Tretiak, S.; Blanchard-Desce, M. Effects of (multi)branching of dipolar chromophores on photophysical properties and two-photon absorption. *J. Phys. Chem. A* **2005**, *109*, 3024.
- (26) Katan, C.; Terenziani, F.; Droumaguet, C. L.; Mongin, O.; Werts, M. H. V.; Tretiak, S.; Blanchard-Desce, M. Branching of dipolar chromophores: effects on linear and nonlinear optical properties. *Proc. SPIE, Int. Soc. Opt. Eng.* **2005**, *5935*, 593503.
- (27) Terenziani, F.; Morone, M.; Gmouh, S.; Blanchard-Desce, M. Linear and Two-Photon Absorption Properties of Interacting Polar Chromophores: Standard and Unconventional Effects. *ChemPhysChem* **2006**, *7*, 685.
- (28) Allain, C.; Schmidt, F.; Lartia, R.; Bordeau, G.; Fiorini-Debuisschert, C.; Charra, F.; Tauc, P.; Teulade-Fichou, M.-P. Vinyl-Pyridinium Triphenylamines: Novel Far-Red Emitters with High Photostability and Two-Photon Absorption Properties for Staining DNA. *ChemBioChem* **2007**, *8*, 424.
- (29) Terenziani, F.; Le Droumaguet, C.; Katan, C.; Mongin, O.; Blanchard-Desce, M. Effect of branching on two-photon absorption in triphenylbenzene derivatives. *ChemPhysChem* **2007**, *8*, 723.
- (30) Kim, H. M.; Seo, M. S.; Jeon, S.-J.; Cho, B. R. Two-photon absorption properties of hexa-substituted benzene derivatives. Comparison between dipolar and octupolar molecules. *Chem. Commun.* **2009**, 7422.
- (31) Katan, C.; Tretiak, S.; Even, J. Two-photon transitions in triazole based quadrupolar and octupolar chromophores: a TD-DFT investigation. *Proc. SPIE, Int. Soc.* , *20* (10), 7712, 77123D.
- (32) Drobizhev, M.; Karotki, A.; Dzenis, Y.; Rebane, A.; Suo, Z. Y.; Spangler, C. W. Strong cooperative enhancement of two-photon absorption in dendrimers. *J. Phys. Chem. B* **2003**, *107*, 7540.
- (33) Yoo, J.; Yang, S. K.; Jeong, M. Y.; Ahn, H. C.; Jeon, S. J.; Cho, B. R. Bis-1,4(p-diarylaminoaryl)-2,5-dicyanobenzene derivatives with large two-photon absorption cross-sections. *Org. Lett.* **2003**, *5*, 645.
- (34) Mongin, O.; Porres, L.; Katan, C.; Pons, T.; Mertz, J.; Blanchard-Desce, M. Synthesis and two-photon absorption of highly soluble three-branched fluorenylene-vinylenes derivatives. *Tetrahedron Lett.* **2003**, *44*, 8121.
- (35) Bartholomew, G. P.; Rumi, M.; Pond, S. J. K.; Perry, J. W.; Tretiak, S.; Bazan, G. C. Two-photon absorption in three-dimensional chromophores based on 2,2 -paracyclophane. *J. Am. Chem. Soc.* **2004**, *126*, 11529.
- (36) Varnavski, O.; Yan, X. Z.; Mongin, O.; Blanchard-Desce, M.; Goodson, T.; Goodson, T. Strongly interacting organic conjugated dendrimers with enhanced two-photon absorption. *J. Phys. Chem. C* **2007**, *111*, 149.
- (37) Katan, C.; Tretiak, S.; Werts, M. H. V.; Bain, A. J.; Marsh, R. J.; Leonczek, N.; Nicolaou, N.; Badaeva, E.; Mongin, O.; Blanchard-Desce, M. Two-photon transitions in quadrupolar and branched chromophores: Experiment and theory. *J. Phys. Chem. B* **2007**, *111*, 9468.
- (38) Rumi, M.; Pond, S. J. K.; Meyer-Friedrichsen, T.; Zhang, Q.; Bishop, M.; Zhang, Y.; Barlow, S.; Marder, S. R.; Perry, J. W. Tetrastyrylarene Derivatives: Comparison of One- and Two-Photon Spectroscopic Properties with Distyrylarene Analogues. *J. Phys. Chem. C* **2008**, *112*, 8061.
- (39) Varnavski, O. P.; Ostrowski, J. C.; Sukhomlinova, L.; Twieg, R. J.; Bazan, G. C.; Goodson, T. Coherent Effects in Energy Transport in Model Dendritic Structures Investigated by Ultrafast Fluorescence Anisotropy Spectroscopy. *J. Am. Chem. Soc.* **2002**, *124*, 1736.
- (40) Parent, M. Ph.D. Thesis, University of Rennes, Rennes, France, 2008.
- (41) Blanchard-Desce and Coll. Unpublished.
- (42) Terenziani, F.; Painelli, A.; Katan, C.; Charlott, M.; Blanchard-Desce, M. Charge instability in quadrupolar chromophores: Symmetry breaking and solvatochromism. *J. Am. Chem. Soc.* **2006**, *128*, 15742.
- (43) Lambert, C.; Schmalzlin, E.; Meerholz, K.; Brauchle, C. Synthesis and nonlinear optical properties of three-dimensional phosphonium ion chromophores. *Chem.—Eur. J.* **1998**, *4*, 512.
- (44) Tretiak, S.; Chernyak, V.; Mukamel, S. Localized Electronic Excitations in Phenylacetylene Dendrimers. *J. Phys. Chem. B* **1998**, *102*, 3310.
- (45) Poliakov, E. Y.; Chernyak, V.; Tretiak, S.; Mukamel, S. Exciton-scaling and optical excitations of self-similar phenyl-acetylene dendrimers. *J. Chem. Phys.* **1999**, *110*, 8161.
- (46) Chernyak, V.; Poliakov, E. Y.; Tretiak, S.; Mukamel, S. Two-exciton states and spectroscopy of phenylacetylene dendrimers. *J. Chem. Phys.* **1999**, *111*, 4158.
- (47) Beljonne, D.; Wenseleers, W.; Zojer, E.; Shuai, Z. G.; Vogel, H.; Pond, S. J. K.; Perry, J. W.; Marder, S. R.; Bredas, J. L. Role of dimensionality on the two-photon absorption response of conjugated molecules: The case of octupolar compounds. *Adv. Funct. Mater.* **2002**, *12*, 631.
- (48) Casida, M. E.; Jamorski, C.; Casida, K. C.; Salahub, D. R. Molecular excitation energies to high-lying bound states from time-dependent density-functional response theory: Characterization and correction of the time-dependent local density approximation ionization threshold. *J. Chem. Phys.* **1998**, *108*, 4439.
- (49) Furche, F.; Ahlrichs, R. Adiabatic time-dependent density functional methods for excited state properties. *J. Chem. Phys.* **2002**, *117*, 7433.
- (50) Grimme, S. Calculation of the electronic spectra of large molecules. In *Reviews in Computational Chemistry*; Lipkowitz, K. B., Boyd, D. B., Eds.; VCH Publishers: New York, 2004; Vol. 20, pp 153–218.
- (51) Dreuw, A.; Head-Gordon, M. Single-reference ab initio methods for the calculation of excited states of large molecules. *Chem. Rev.* **2005**, *105*, 4009.
- (52) Champagne, B.; Guillaume, M.; Zutterman, F. TDDFT investigation of the optical properties of cyanine dyes. *Chem. Phys. Lett.* **2006**, *425*, 105.

- (53) Miura, M.; Aoki, Y.; Champagne, B. Assessment of time-dependent density functional schemes for computing the oscillator strengths of benzene, phenol, aniline, and fluorobenzene. *J. Chem. Phys.* **2007**, *127*, 084103.
- (54) Magyar, R. J.; Tretiak, S. Dependence of spurious charge-transfer excited states on orbital exchange in TDDFT: Large molecules and clusters. *J. Chem. Theory Comput.* **2007**, *3*, 976.
- (55) Jacquemin, D.; Wathélet, V.; Perpète, E. A.; Adamo, C. Extensive TD-DFT Benchmark: Singlet-Excited States of Organic Molecules. *J. Chem. Theory Comput.* **2009**, *5*, 2420.
- (56) Tretiak, S.; Chernyak, V. Resonant nonlinear polarizabilities in the time-dependent density functional theory. *J. Chem. Phys.* **2003**, *119*, 8809.
- (57) Masunov, A.; Tretiak, S. Prediction of two-photon absorption properties for organic chromophores using time-dependent density-functional theory. *J. Phys. Chem. B* **2003**, *108*, 899.
- (58) Kobko, N.; Masunov, A.; Tretiak, S. Calculations of the third-order nonlinear optical responses in push-pull chromophores with a time-dependent density functional theory. *Chem. Phys. Lett.* **2004**, *392*, 444.
- (59) Kauffman, J. F.; Turner, J. M.; Alabugin, I. V.; Breiner, B.; Kovalenko, S. V.; Badaeva, E. A.; Masunov, A.; Tretiak, S. Two-photon excitation of substituted enediynes. *J. Phys. Chem. A* **2005**, *110*, 241.
- (60) Badaeva, E. A.; Timofeeva, T. V.; Masunov, A.; Tretiak, S. Role of donor-acceptor strengths and separation on the two-photon absorption response of cytotoxic dyes: A TD-DFT study. *J. Phys. Chem. A* **2005**, *109*, 7276.
- (61) Clark, A. E. Time-Dependent Density Functional Theory Studies of the Photoswitching of the Two-Photon Absorption Spectra in Stilbene, Metacyclopheadiene, and Diarylethene Chromophores. *J. Phys. Chem. A* **2006**, *110*, 3790.
- (62) Wu, C.; Tretiak, S.; Chernyak, V. Y. Excited states and optical response of a donor–acceptor substituted polyene: A TD-DFT study. *Chem. Phys. Lett.* **2007**, *433*, 305.
- (63) Katan, C.; Charlot, M.; Mongin, O.; Le Droumaguet, C. I.; Jouikov, V.; Terenziani, F.; Badaeva, E.; Tretiak, S.; Blanchard-Desce, M. Simultaneous Control of Emission Localization and Two-Photon Absorption Efficiency in Dissymmetrical Chromophores. *J. Phys. Chem. B* **2010**, *114*, 3152.
- (64) Cross-shaped chromophores consisting of four donor substituted branches linked to an aromatic core have already been investigated but show significant differences, e.g., in OPA spectra, and can well be described as a dimer of corresponding quadrupolar benchmarks.<sup>38</sup>
- (65) Ultrafast fluorescence spectroscopy has already been performed on a related carbon-cored tetramer.<sup>39</sup>
- (66) Frisch, M. J.; Trucks, G. W.; Schlegel, H. B.; Scuseria, G. E.; Robb, M. A.; Cheeseman, J. R.; Montgomery, J. A., Jr.; Stratmann, R. E.; Burant, J. C.; Dapprich, S.; Millam, J. M.; Daniels, A. D.; Kudin, K. N.; Strain, M. C.; Farkas, O.; Tomasi, J.; Barone, V.; Cossi, M.; Cammi, R.; Mennucci, B.; Pomelli, C.; Adamo, C.; Clifford, S.; Ochterski, J.; Petersson, G. A.; Ayala, P. Y.; Cui, Q.; Morokuma, K.; Malick, D. K.; Rabuck, A. D.; Raghavachari, K.; Foresman, J. B.; Cioslowski, J.; Ortiz, J. V.; Stefanov, B. B.; Liu, G.; Liashenko, A.; Piskorz, P.; Komaromi, I.; Martin, R. L.; Fox, D. J.; Keith, T.; Al-Laham, M. A.; Peng, C. Y.; Nanayakkara, A.; Challacombe, M.; Gill, P. M. W.; Johnson, B.; Chen, W.; Wong, M. W.; Gonzalez, C.; Pople, J. A. *Gaussian 03*, revision D.02; Gaussian, Inc.: Wallingford, CT, 2004.
- (67) Frisch, M. J.; Trucks, G. W.; Schlegel, H. B.; Scuseria, G. E.; Robb, M. A.; Cheeseman, J. R.; Montgomery, J. A., Jr.; Vreven, T.; Kudin, K. N.; Burant, J. C.; Millam, J. M.; Iyengar, S. S.; Tomasi, J.; Barone, V.; Mennucci, B.; Cossi, M.; Scalmani, G.; Rega, N.; Petersson, G. A.; Nakatsuji, H.; Hada, M.; Ehara, M.; Toyota, K.; Fukuda, R.; Hasegawa, J.; Ishida, M.; Nakajima, T.; Honda, Y.; Kitao, O.; Nakai, H.; Klene, M.; Li, X.; Knox, J. E.; Hratchian, H. P.; Cross, J. B.; Bakken, V.; Adamo, C.; Jaramillo, J.; Gomperts, R.; Stratmann, R. E.; Yazyev, O.; Austin, A. J.; Cammi, R.; Pomelli, C.; Ochterski, J. W.; Ayala, P. Y.; Morokuma, K.; Voth, G. A.; Salvador, P.; Dannenberg, J. J.; Zakrzewski, V. G.; Dapprich, S.; Daniels, A. D.; Strain, M. C.; Farkas, O.; Malick, D. K.; Rabuck, A. D.; Raghavachari, K.; Foresman, J. B.; Ortiz, J. V.; Cui, Q.; Baboul, A. G.; Clifford, S.; Cioslowski, J.; Stefanov, B. B.; Liu, G.; Liashenko, A.; Piskorz, P.; Komaromi, I.; Martin, R. L.; Fox, D. J.; Keith, T.; Al-Laham, M. A.; Peng, C. Y.; Nanayakkara, A.; Challacombe, M.; Gill, P. M. W.; Johnson, B.; Chen, W.; Wong, M. W.; Gonzalez, C.; Pople, J. A. *Gaussian 03*, revision D.02; Gaussian, Inc.: Wallingford, CT, 2004.
- (68) Martin, R. L. Natural transition orbitals. *J. Chem. Phys.* **2003**, *118*, 4775.
- (69) Kokalj, A. Computer graphics and graphical user interfaces as tools in simulations of matter at the atomic scale. *Comput. Mater. Sci.* **2003**, *28*, 155.
- (70) Mongin, O.; Porres, L.; Charlot, M.; Katan, C.; Blanchard-Desce, M. Synthesis, fluorescence, and two-photon absorption of a series of elongated rodlike and banana-shaped quadrupolar fluorophores: A comprehensive study of structure-property relationships. *Chem.—Eur. J.* **2007**, *13*, 1481.
- (71) Lu, D.; Chen, G.; Perry, J. W.; Goddard, W. A. Valence-Bond Charge-Transfer Model For Nonlinear-Optical Properties Of Charge-Transfer Organic-Molecules. *J. Am. Chem. Soc.* **1994**, *116*, 10679.
- (72) Barzoukas, M.; Blanchard-Desce, M. Molecular engineering of push-pull dipolar and quadrupolar molecules for two-photon absorption: A multivalence-bond states approach. *J. Chem. Phys.* **2000**, *113*, 3951.
- (73) Terenziani, F.; Sissa, C.; Painelli, A. Symmetry breaking in octupolar chromophores: Solvatochromism and electroabsorption. *J. Phys. Chem. B* **2008**, *112*, 5079.
- (74) Allen, F. H. The Cambridge Structural Database: a quarter of a million crystal structures and rising. *Acta Crystallogr., Sect. B: Struct. Sci.* **2002**, *58*, 380.
- (75) Basavoju, S.; Aitipamula, S.; Desiraju, G. R. Host-guest and network structures of some tetraphenylmethane derivatives. *CrystEngComm.* **2004**, *6*, 120.
- (76) Oldham, W. J.; Lachicotte, R. J.; Bazan, G. C. Synthesis, spectroscopy, and morphology of tetrastilbenoidmethanes. *J. Am. Chem. Soc.* **1998**, *120*, 2987.
- (77) Porres, L.; Mongin, O.; Katan, C.; Charlot, M.; Pons, T.; Mertz, J.; Blanchard-Desce, M. Enhanced two-photon absorption with novel octupolar propeller-shaped fluorophores derived from triphenylamine. *Org. Lett.* **2004**, *6*, 47.